

## Hydrogen Bonding with Sulfur

Matthew K. Krepps, Sean Parkin, and David A. Atwood\*

Department of Chemistry, The University of Kentucky, Lexington, Kentucky 40506-0055

Received February 5, 2001; Revised Manuscript Received May 24, 2001

**ABSTRACT:** The hydrogen-bonding capabilities of the sulfur-containing molecule trimercaptotriazine (TMT) was explored using various amines. The amines were chosen to observe the effect of varying base strength on the resulting hydrogen-bonded structures. The specific compounds [pyrrolidineH]<sup>+</sup><sub>2</sub>[HTMT]<sup>2-</sup>·THF (**1**), [triethylamineH]<sup>+</sup>[H<sub>2</sub>TMT]<sup>-</sup>·THF (**2**), [propylenediamineH<sub>2</sub>]<sup>2+</sup>[HTMT]<sup>2-</sup> (**3**), [ethylenediamineH]<sup>+</sup><sub>2</sub>[HTMT]<sup>2-</sup> (**4**), and [pyridineH]<sup>+</sup>[H<sub>2</sub>TMT]<sup>-</sup>(H<sub>3</sub>TMT·2(pyridine)) (**5**) were characterized by melting point, elemental analysis, infrared spectroscopy, and X-ray crystallography. It was found that the TMT molecule is readily deprotonated by all of the amines and that the subsequent ammonium hydrogens formed several types of hydrogen bonds. Importantly, these bonds were observed to form with the sulfur atoms of the TMT, with S···N distances of 3.3–3.5 Å.

### Introduction

Supramolecular chemistry is both ancient and new. It is ancient in that the origins of life may have begun through self-organized weak interactions. An understanding of the guiding principles behind the chemistry is, however, a new and continuing development.<sup>1,2</sup> One of the predominant interactions is the hydrogen bond. These three-center–two-electron bonds form between protic hydrogens and proximal electron-rich atoms, usually oxygen, nitrogen, or chlorine. Given the slight electronegativity difference between H and S ( $\delta$  0.38, Pauling scale), it is likely that hydrogen bonding involving sulfur and hydrogen could occur. Such bonds would necessarily be weak, due to the poorer match between the hard proton and soft sulfur. Surprisingly, little work has been done in this area, however, with only sporadic reports of S···H hydrogen bonding.<sup>3–5</sup> For instance, this contact has been observed in Allen's compilation and analysis of S···H–N bonds.<sup>6</sup> Living systems contain several important sulfur-containing molecules, including the amino acids cysteine and methionine. A greater understanding of S···H bonding may have fundamental importance in biochemical research in understanding and predicting protein folding and biomolecular interactions.<sup>7</sup>

Several hydrogen-bonded supramolecular studies have focused on molecules with C<sub>3</sub> symmetry, due to their ability to form highly organized, extended structures.<sup>8</sup> In a like manner, the D<sub>3h</sub>-symmetric molecule trimercaptotriazine was used to explore the nature and extent of S···H bonding and implications of this interaction to supramolecular chemistry in hydrogen-bonded complexes with the amines pyrrolidine, triethylamine, propylenediamine, ethylenediamine, and pyridine.

### Results and Discussion

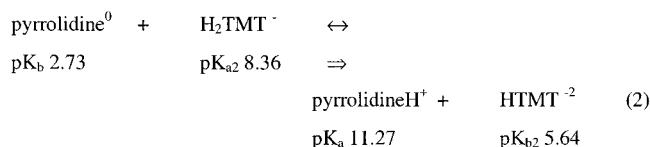
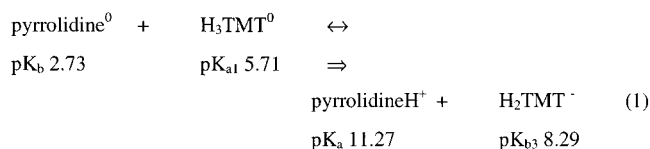
**Synthesis and Spectroscopy.** One, two, and three moles of an amine (in order of decreasing base strength, Table 1) were added to a solution of H<sub>3</sub>TMT in thf. Not all of the resulting complexes could be definitively characterized. However, in all cases it was found that the added base formed some type of complex with the

Table 1. pK<sub>b</sub> Values<sup>a</sup> of Selected Amines

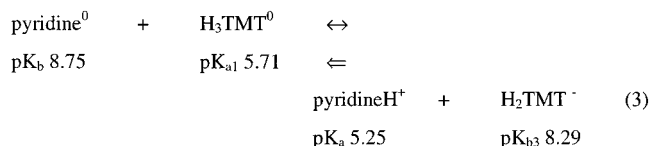
	amine	pK <sub>b</sub>	temp (°C)
<b>1</b>	pyrrolidine	2.73	25
<b>2</b>	triethylamine	2.99	18
<b>3</b>	propylenediamine		
	first	3.06	10
	second	4.97	10
<b>4</b>	ethylenediamine		
	first	3.29	0
	second	6.44	0
<b>5</b>	pyridine	8.75	25

<sup>a</sup> All values measured from an aqueous solution at the given temperature.

deprotonated TMT molecule (pK<sub>a1</sub> = 5.71, pK<sub>a2</sub> = 8.36, pK<sub>a3</sub> = 11.38)<sup>9</sup>. In the case of **1** an amine:TMT ratio of 2:1 and 3:1 led to the same product. For **2** and **5**, ratios of 1:1, 2:1, and 3:1 led to the same product. In **3** only, the stoichiometry of the reactants followed the stoichiometry in the product. In the case of **4** a 1:1 addition forms the 2:1 complex. In these compounds, the strength of the base is important (Table 1). For example, pyrrolidine, a strong base, can abstract two protons from the TMT molecule, while pyridine, a much weaker base, is able to extract only one proton from a TMT molecule. Since propylenediamine and ethylenediamine have the potential to extract two protons, it is not clear why the addition of three triethylamine molecules leads to only a single deprotonation. It is possible that the sterics associated with additional triethylamine molecules would disrupt the TMT two-dimensional aggregation (see Figure 6). The triply deprotonated TMT<sup>3-</sup> was not found to occur. While the pK<sub>a</sub> value of this third proton has recently been found (pK<sub>a3</sub> = 11.38), it is certainly too large for deprotonation by the five bases used.<sup>9</sup> Thus, the formation of these compounds can, with the exception of the relatively sterically bulky triethylamine, be explained simply on the basis of amine base strength and without regard to reactant ratio. Take, for example, the acid–base reactions of pyrrolidine, the strongest base, and H<sub>3</sub>TMT (reactions 1 and 2). By comparing the pK<sub>b</sub> and pK<sub>a</sub> values in the equations, it becomes easy to see that pyrrolidine should deprotonate H<sub>3</sub>TMT twice to form the dianionic compound [pyrrolidineH]<sup>+</sup><sub>2</sub>[HTMT]<sup>2-</sup>·THF (**1**). In contrast, the acid–base reaction



of the weak base pyridine and  $\text{H}_3\text{TMT}$  results in a single deprotonation only a portion of the time (reaction 3).



Reaction 3 lies only slightly to the left; therefore, both sets of species are found in the crystal, the ion pair  $[\text{pyridineH}^+][\text{H}_2\text{TMT}]^-$  and the coordinated group  $\text{H}_3\text{TMT} \cdot 2(\text{pyridine})$ .

The molecular formulas of the complexes could be ascertained by elemental analyses. However, this was a challenging task, for the compounds were solvated with thf, which was easily lost during sample preparation and analysis. The presence of various types of TMT molecules and ammonium hydrogens could be determined by the infrared data. It had previously been established that strong absorptions for uncoordinated  $\text{H}_3\text{TMT}$  occur at 1540, 1125, and 745  $\text{cm}^{-1}$  and are characteristic of the nonaromatic, trithione form of the TMT ring system (Figure 1a).<sup>10</sup> The aromatic, trithiol form of the ring (Figure 1b), on the other hand, was characterized by the presence of three strong absorptions located at 1490, 1245, and 860  $\text{cm}^{-1}$ . These were observed, for example, in the spectrum of  $(\text{CH}_3)_3\text{TMT}$  (Figure 1b)<sup>11</sup> and transition-metal compounds of the formula  $\text{M}_3(\text{TMT})_2$  ( $\text{M} = \text{Co}, \text{Cu}$ ).<sup>12</sup> However, in compounds having the formulas  $\text{M}(\text{HTMT})$  and  $\text{M}(\text{H}_2\text{TMT})_2$  resonances for both forms of the ligand were observed.<sup>13</sup> More specifically, the IR of  $\text{NaH}_2\text{TMT} \cdot 3\text{H}_2\text{O}$ , whose crystal structure has been determined, exhibits vibrations at 1484, 1241, and 883  $\text{cm}^{-1}$  and at 1558, 1151, and 781  $\text{cm}^{-1}$ .<sup>14</sup> In all five compounds presented here, the IR shows both sets of absorptions, indicating a structural form somewhere between the thione and thiol.

Evidence that the hydrogen atoms of  $\text{HTMT}^{2-}$  and  $\text{H}_2\text{TMT}^-$  are located on the nitrogen atoms is provided, in part, by the presence of bands assigned to N–H stretching vibrations in the 2860–3100  $\text{cm}^{-1}$  range for **1–5**. This is below the amine and ammonium absorptions ( $\sim 3400 \text{ cm}^{-1}$ ). With the overlap of C–H vibrations in the same region, careful investigation was necessary for accurate assignment. For instance, in compound **5**, pyridine is H-bonded to  $\text{H}_2\text{TMT}^-$ . The IR spectrum of neat pyridine displays four peaks between 3000 and 3080  $\text{cm}^{-1}$ . However, the IR of **5**, while including these peaks, shows an additional broad peak at 2877  $\text{cm}^{-1}$ . This is assigned to the N–H stretching. The lower than normal wavenumber for the N–H stretch is indicative of a weaker hydrogen bond.

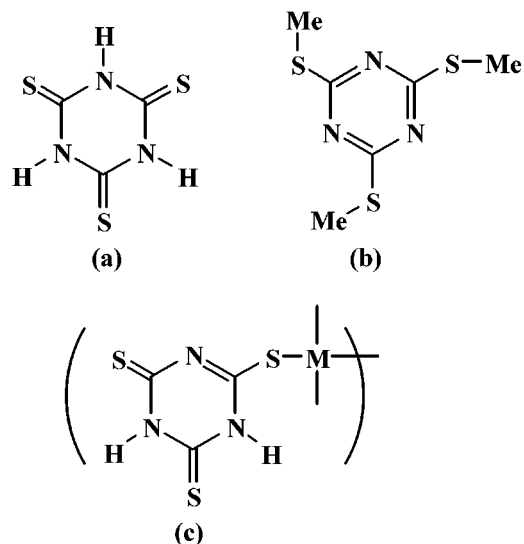


**Figure 1.** TMT in the thione (a), thiol (b), and metalated (c) forms.

Previous studies have shown that the longer the C=S bond length, the more likely a hydrogen bond is to form. The C=S bond can be lengthened by placing one or more nitrogen atoms on the thione carbon ( $\text{R}_2\text{C}=\text{S} = 1.58 \text{ \AA}$  to  $\text{R}'_2\text{C}=\text{S} = 1.75 \text{ \AA}$  where  $\text{R} = \text{C}_{\text{sp}^3}$  and  $\text{R}' = \text{N}$ ). Placing one or more nitrogens on the thiol carbon causes the effective electronegativity of the S to be increased by conjugative interactions between the C=S and the lone pair(s) of the N.<sup>6</sup> Accordingly, the bond length of the C=S unit in the TMT molecules of compounds **1–5** that are involved in hydrogen bonding are approximately 1.7(1)  $\text{Å}$ .

It has been previously suggested that as the  $\text{S} \cdots \text{H}-\text{N}$  (or  $\text{N} \cdots \text{H}-\text{N}$ ) bond angle approaches  $180^\circ$ , the hydrogen-bond distance ( $\text{S} \cdots \text{H}$  or  $\text{N} \cdots \text{H}$ ) decreases and therefore strengthens.<sup>6</sup> Crystal structures of **1–5** are consistent with this conclusion. Bond angles for  $\text{S} \cdots \text{H}-\text{N}$  (or  $\text{N} \cdots \text{H}-\text{N}$ ) in these compounds range from 158.1 to 173.7(1) $^\circ$  and show the direct correlation that increasing the bond angle results in a shortening, and therefore strengthening, of the hydrogen bond (Table 2). Therefore, the resulting  $\text{S} \cdots \text{H}-\text{N}$  hydrogen-bond distances of 2.37–2.48  $\text{Å}$  coincide with fairly strong to medium hydrogen bonds according to the published literature.<sup>15,16</sup>

**Structural Characterization.** TMT was chosen as a substrate since the  $D_{3h}$  symmetry of the molecule (fully deprotonated) could provide a potential point of organization for the formation of supramolecular assemblies. Additionally, the existence of hydrogen bonding, including  $\text{S} \cdots \text{H}$  bonding, had already been demonstrated within the TMT–base system (base = thf, dioxane)<sup>4</sup> and in some structurally characterized compounds of TMT with the group 2 elements.<sup>17</sup> The main structural unit in these compounds comprised adjacent TMT molecules with complementary N–H $\cdots$ S hydrogen bonding (Figure 2; note that  $\text{H}_3\text{TMT}$  exists in the thione form). Secondly, the TMT molecules may pack in an efficient manner in what appears to be a face-to-face  $\pi$  stacking (Figure 2).<sup>18</sup> The adjacent hydrogen bonding also exists in cyanuric acid, which has been used in combination with complementary molecules to produce two-dimensional supramolecular arrays.<sup>19</sup> To explore

**Table 2.** Compilation of the Hydrogen-Bonding Contacts<sup>a</sup> in **1–5**

compd	type I S···H–N		type II S···H–N (am)		type III N···H–N (am)		type IV N···H–N (TMT)	
	S···N	S···H	S···N	S···H	N···N	N···H	N···N	N···H
<b>1</b>	3.315(2)	2.44	3.269(2)	2.37	2.800–2.844(3)	1.89–1.94		
<b>2</b>	3.304–3.337(2)	2.44–2.48			2.852(3)	1.93		
<b>3</b>	3.332(4)	2.47	3.311(4)	2.43	2.777(5)	1.88–1.91		
<b>4</b>			3.316(4)	2.60	2.826(5)			
			3.363–3.553(3)	2.51–2.74	2.808(4)	1.90–1.94	2.893(4)	2.00
<b>5</b>	3.237–3.478(2)	2.37–2.48			2.833(4)			
					2.722(2)	1.87–1.88		
					2.743(2)			

<sup>a</sup> Standard deviations do not exist for the S···H distances, since the H atoms are in calculated positions. Distances are in Å.

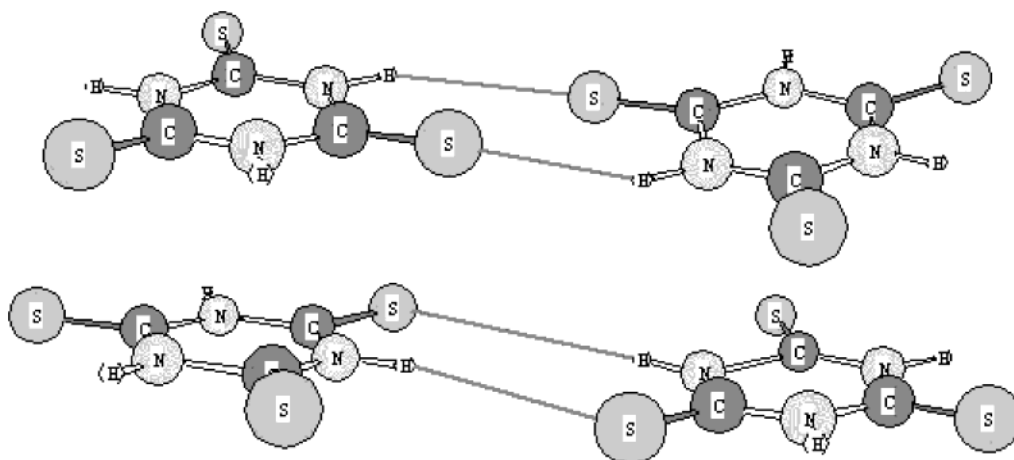


**Figure 2.** Structure of H<sub>3</sub>TMT, comprised of a two-dimensional sheetlike array of hydrogen bonds from the S of one ring to the H–N of an adjacent ring. To form the third dimension, the rings layer themselves face to face, held together by π stacking. Note that in the solid state H<sub>3</sub>TMT is in the thione form.

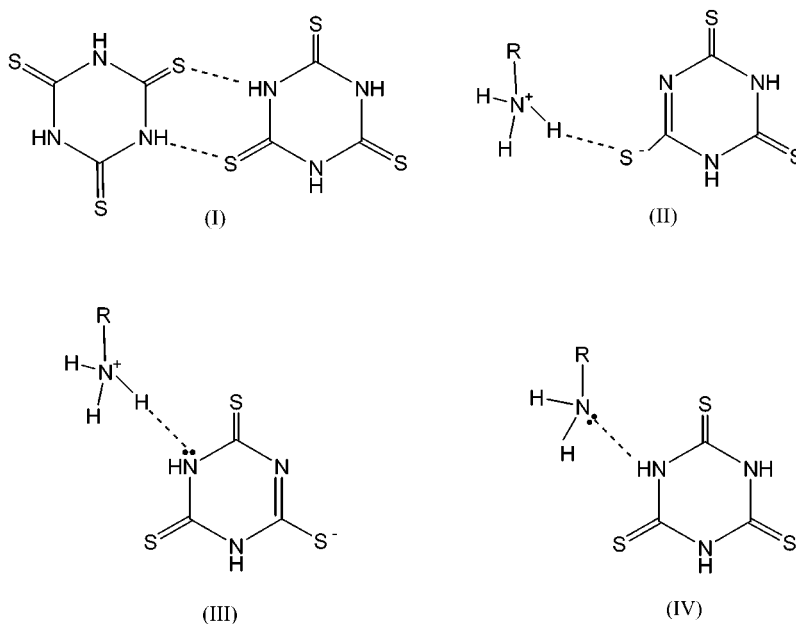


**Figure 3.** Four types of hydrogen bond contacts in compounds **1–5**: (I) contacts between S and H–N on adjacent TMT rings; (II) contacts between S of TMT and H–N of amines; (III) contacts between N of TMT and H–N of amines; (IV) contacts between N and H–N on TMT rings.

the types of hydrogen bonding that might occur between TMT and amine molecules, the structures of **1–5** were determined.

In the structure of **1**, the pyrrolidine molecules abstract two protons from H<sub>3</sub>TMT, leaving HTMT<sup>2-</sup>, which forms three types of hydrogen bonds (Table 2, Figures 3 and 4), adjacent TMT–TMT bonds (type I),

ammonium–sulfur bonds (type II), and amine–ammonium bonds (type III). Additionally, there is an ammonium contact with a thf molecule in the lattice (O···N = 2.805(3) Å, O···H = 1.90 Å). Thus, for one TMT molecule all of the nitrogen atoms and two of the sulfur atoms are involved in hydrogen bonding. Combined, these contacts do not lead to a supramolecular assembly

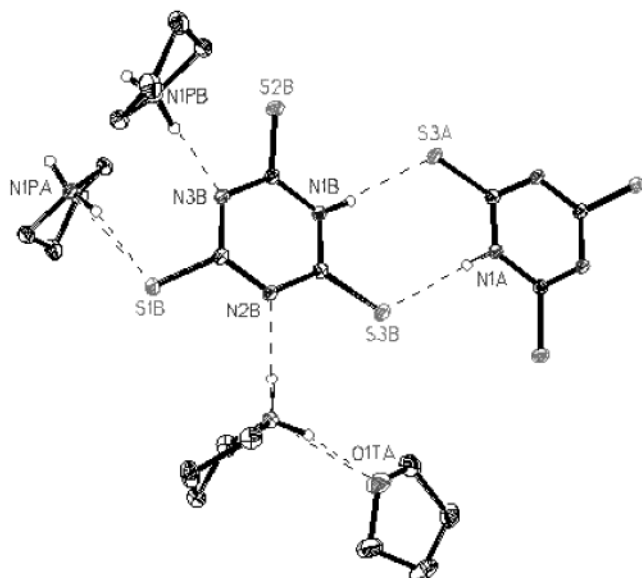


**Figure 4.** Four types of hydrogen bonds adopted by TMT and pyrrolidine: two  $S\cdots N$  and two  $N\cdots N$ .

but, rather, an assortment of hydrogen-bonding contacts involving the TMT unit, the amine, and thf.

Despite the marginally weaker base strength of  $NEt_3$  vs pyrrolidine, only one deprotonation occurs in **2**. The structure is then simplified by the presence of four type I bonds between adjacent TMT units. This structural feature predominates, and a two-dimensional zigzag ribbon structure results (Figure 5). The ribbon is aligned along the  $c$  (long) axis of the unit cell (see the Supporting Information). The ammonium groups (with type II contacts) widen the spacing of the two-dimensional network, making room for uncoordinated thf (Figure 6 (thf not shown for clarity)). It is possible that the presence of two triethylamine units in this structure would disrupt the hydrogen bonding, leading to a less stable structure. Thus, sterics are probably the reason addition of three triethylamine molecules to  $H_3TMT$  leads to only one deprotonation.

This is indirectly verified in the structure of **3**, which contains doubly deprotonated  $HTMT^{2-}$  units, while the base strength of propylenediamine is almost exactly that of triethylamine. The structure of **3** contains pairs of TMT units held together with type I bonding (Figure 7). Both of the amine nitrogens are protonated. Two of the ammonium hydrogens are employed in type II bonding to sulfur, with the third forming a type III bond to a nitrogen on TMT. The hydrogen-bonding contacts combine to produce a complicated three-dimensional array. This is the only structure in this group that demonstrates potential  $\pi$  stacking. The TMT units are arranged such that the interplanar distance between TMT rings is 3.559(4) Å (Figure 8).

In contrast to **3**, the structure of **4** does not possess type I contacts. Type II bonds predominate to both ammonium and amine (the bonds to S3A and S2A, respectively; Figure 9). It is interesting to note that a type IV bond occurs, between a TMTN H and an amine, rather than deprotonation to form a type III bond. A type III contact does exist in the structure, between N1BC and N3B. Overall, these hydrogen bonds form a three-dimensional supramolecular network made up of

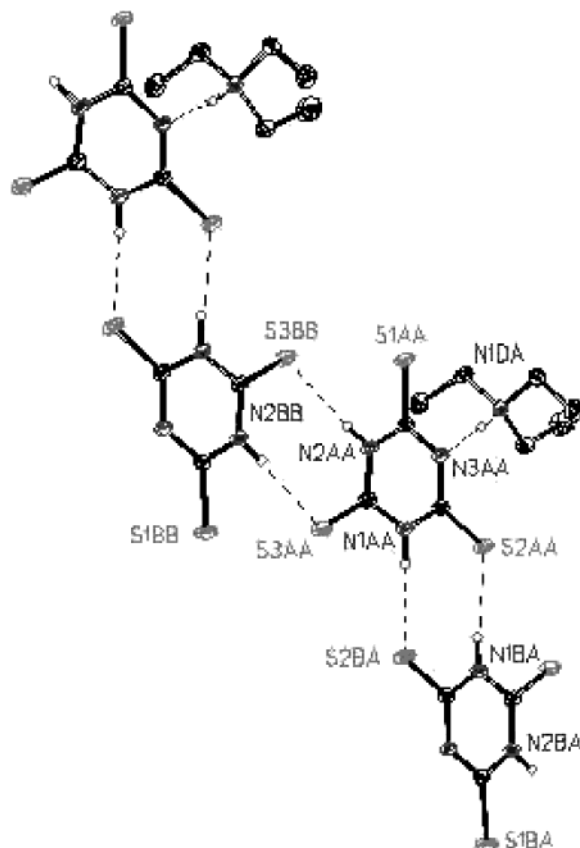


**Figure 5.** The two types of hydrogen bonds formed by  $NEt_3$  and TMT: one type between adjacent TMT rings and one type between TMT and  $NEt_3$ . The hydrogen bonding creates a two-dimensional zigzag structure.

staggered columns of TMT units separated by the ammonium molecules. These are aligned along the  $b$  axis in the unit cell (see Supporting Information).

Like **2**, compound **5** also possesses four type I hydrogen bonds (Figure 10), but they are lined up in more of a linear array along the  $c$  axis in the unit cell. The pyridine deprotonates the TMT once and forms a type III hydrogen bond. A single deprotonation is in keeping with the relative weak base strength of pyridine. This is also reflected in the fact that there is an unprotonated pyridine in the structure as well which forms a type III hydrogen bond with a TMT proton (not shown).

Within the TMT molecules, the C–N (~1.36(1) Å) and C–S (~1.7(1) Å) distances and N–C–S (~118(3)°) and C–N–C (~120(3)°) angles were not unusual.<sup>9,12,14,17</sup> For the amines the C–N and C–C distances fell in the usual range.

## Conclusions

The TMT–amine combinations described herein feature a wide range of hydrogen-bonding contacts. However, the bonds involving TMT (with only one exception, compound **3**) are in one plane, leading to two-dimensional extended structures. The nature of the hydrogen-bonded complexes can be loosely predicted on the basis of the  $pK_b$  values of the base in conjunction with the  $pK_a$  values of  $H_3TMT$ . The only exception is **2**, in which the resulting structure appears to be due to the increased steric bulk of the amine.

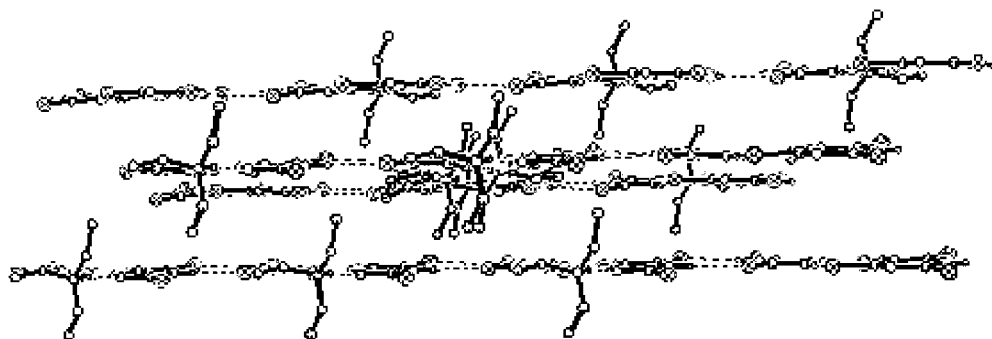


**Figure 6.** The two-dimensional network of **2**. The three R groups on the ammonium ion widen the spacing of the two-dimensional network enough to allow uncoordinated thf to reside within the interlayer.

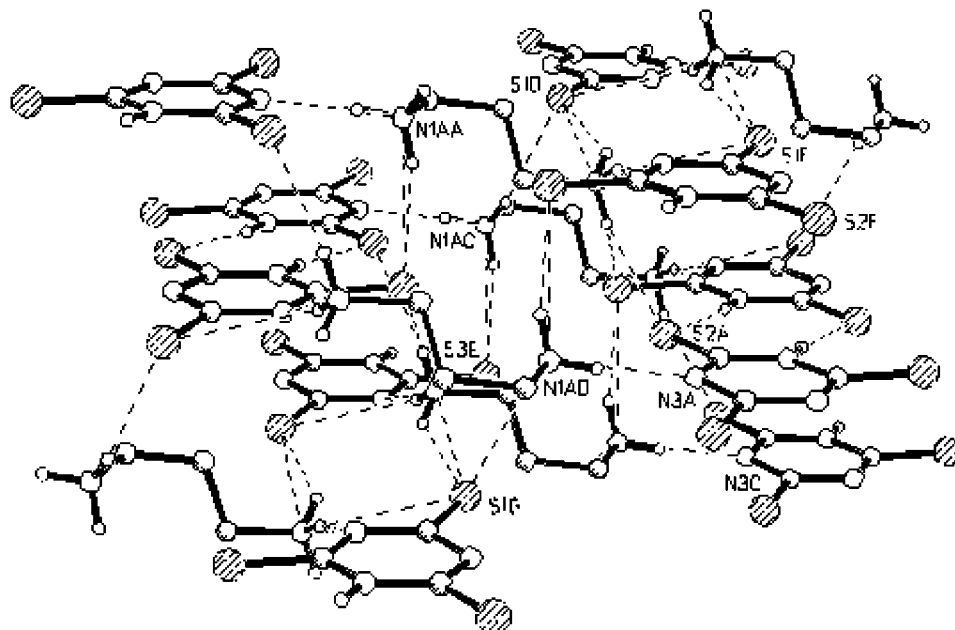


**Figure 7.** The two-dimensional network of **3**. The diamine demonstrates how one molecule can doubly deprotonate a TMT. This may happen if the second  $pK_b$  is sufficiently strong.

The  $S\cdots H-N$  contacts fall within the narrow range (for the  $S\cdots N$  distance) of 3.237(2)–3.553(3) Å. This compares closely to other non-TMT compounds, which feature a similar range of distances: 3.36 Å in methyl dithiocarbazate and 3.0–3.5 Å in the active centers of ferredoxins.<sup>20</sup>

### Experimental Section

**General Considerations.** All manipulations were conducted on the benchtop using clean, oven-dried glassware. All solvents were rigorously dried prior to use.  $Na_3TMT \cdot 9H_2O$  was obtained from Degussa Corp. and then purified as reported previously.<sup>17</sup>  $H_3TMT$  was obtained by treating  $Na_3TMT \cdot 9H_2O$  with concentrated hydrochloric acid in a 1:3 molar ratio. In a typical reaction, 100 g of  $Na_3TMT \cdot 9H_2O$  was dissolved in 350 mL of water and the solution filtered. To the filtrate was added 61 mL of concentrated hydrochloric acid (12.1 N). A yellow precipitate formed immediately. The mixture was stirred briefly and the precipitate isolated by filtration, washed with water, and dried, first at room temperature and then at 110 °C. The typical yield is about 40 g (91%). A stock solution of  $H_3TMT$  in THF was produced to facilitate consistent concentrations of  $H_3TMT$  when combined in solution with the various amines. The concentration of the light yellow  $H_3TMT/THF$  solution was found to be 116.8 mM (1.035 g/50 mL, 5.839 mmol/50 mL). The stock solution was stored in a tightly sealed brown jug prior to use.

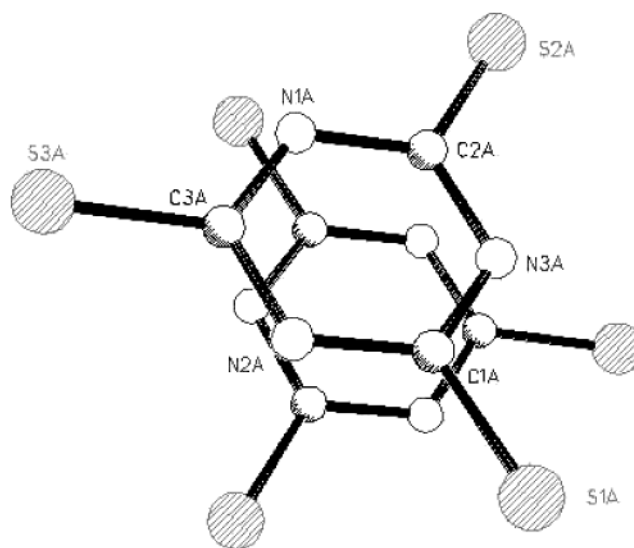


**Figure 8.** Structure of compound **3**. This is the only structure that demonstrates potential  $\pi$  stacking similar to the crystal structure of  $H_3TMT$ .

All X-ray analyses were conducted on X-ray-quality crystals. Analytical data were collected on both powder and crystalline

Table 3. X-ray Data Collection and Structure Analysis Details for Compounds 1–5

	1	2	3	4	5
empirical formula	C <sub>15</sub> H <sub>29</sub> N <sub>5</sub> OS <sub>3</sub>	C <sub>26</sub> H <sub>52</sub> N <sub>8</sub> O <sub>2</sub> S <sub>6</sub>	C <sub>6</sub> H <sub>12</sub> N <sub>5</sub> S <sub>3</sub>	C <sub>7</sub> H <sub>19</sub> N <sub>7</sub> S <sub>3</sub>	C <sub>24</sub> H <sub>24</sub> N <sub>12</sub> S <sub>9</sub>
fw	391.61	701.12	250.39	297.47	769.09
temp (K)	173(1)	173(1)	144(1)	173(1)	173(1)
cryst syst	triclinic	triclinic	triclinic	monoclinic	triclinic
space group	<i>P</i> $\bar{1}$	<i>P</i> $\bar{1}$	<i>P</i> $\bar{1}$	<i>P</i> 2 <sub>1</sub> / <i>c</i>	<i>P</i> $\bar{1}$
unit cell dimens					
<i>a</i> (Å)	8.6460(17)	10.5580(10)	6.820(2)	4.7440(10)	10.8220(10)
<i>b</i> (Å)	8.7020(17)	11.2920(10)	9.257(2)	33.520(3)	12.8090(10)
<i>c</i> (Å)	14.127(3)	16.629(2)	9.867(2)	8.709(2)	12.9930(10)
α (deg)	89.48(3)	79.153(10)	115.631(10)	90	82.598(10)
β (deg)	72.49(3)	73.444(10)	97.157(10)	99.955(10)	85.717(10)
γ (deg)	80.04(3)	85.882(10)	94.338(10)	90	70.406(10)
<i>V</i> (Å <sup>3</sup> )	997.3(3)	1866.0(3)	551.4(2)	1364.0(4)	1681.7(2)
<i>Z</i>	2	2	2	4	2
<i>D</i> <sub>calcd</sub> (g/cm <sup>3</sup> )	1.304	1.248	1.508	1.449	1.519
abs coeff (mm <sup>-1</sup> )	0.384	0.401	0.642	0.535	0.632
goodness of fit on <i>F</i> <sup>2</sup>	1.043	1.099	1.037	1.054	1.038
final <i>R</i> <sub>1</sub> , <i>wR</i> <sub>2</sub> ( <i>I</i> > 2σ( <i>I</i> ))	0.0449, 0.0973	0.0518, 0.1316	0.0337, 0.0768	0.0255, 0.0614	0.0340, 0.0779

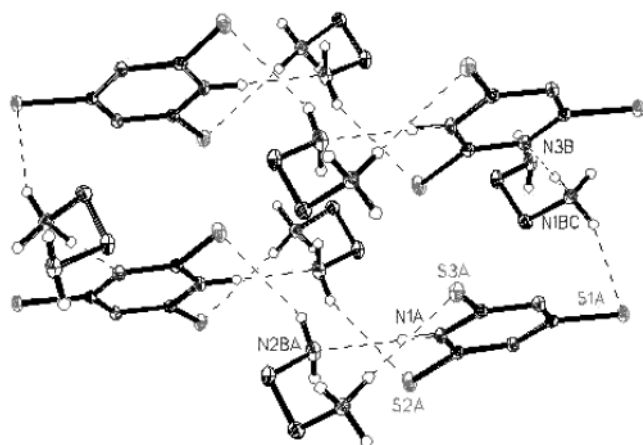


**Figure 9.** The three-dimensional network of **4**, including the diamine, ethylenediamine, which is only monoprotonated. The second *pK<sub>b</sub>* is apparently too weak to doubly deprotonate the TMT ring.

samples and were found to be identical. Elemental analyses were obtained on an Elementar III analyzer. Infrared data were recorded as KBr pellets on a Matheson Instruments 2020 Galaxy Series spectrometer and are reported in cm<sup>-1</sup>. Both EA and IR data were collected on samples that had been air-dried for at least 24 h. Melting point data were taken on crystalline samples in sealed glass capillaries.

X-ray diffraction data were collected at 173 K (**1**, **2**, **4**, and **5**) and 144 K (**3**) on a Nonius Kappa-CCD diffractometer from irregular-shaped crystals. The structures were solved by direct methods (SHELXS97)<sup>21</sup> and interpretation of difference Fourier maps (SHELXL97). Refinement was carried out against *F*<sup>2</sup> by weighted full-matrix least squares (SHELXL97). All hydrogen atoms were found in difference maps and subsequently placed at calculated positions and refined using a riding model with *U*<sub>iso</sub> tied to the corresponding heavy atom. Non-hydrogen atoms were refined with anisotropic displacement parameters. Atomic scattering factors were taken from ref 22. Spatial variation in the *R* value as a function of position in reciprocal space was checked by the *R*-Tensor method.<sup>23</sup> X-ray data collection and structure refinement details for compounds **1**–**5** are given in Table 3.

**General Synthesis of [Amine]<sup>+</sup>[TMT]<sup>-</sup>.** A 50.0 mL portion of stock solution (5.839 mmol of H<sub>3</sub>TMT) was added to a beaker. A glass syringe was used to introduce 5.839, 11.678, or 17.517 mmol of the amine, which corresponds to a molar ratio of 1:1, 2:1, or 3:1, respectively. The solution was stirred briefly with a glass rod, and the mixture was covered tightly with aluminum foil. The solutions were allowed to evaporate slowly and were undisturbed until crystals formed. Some of

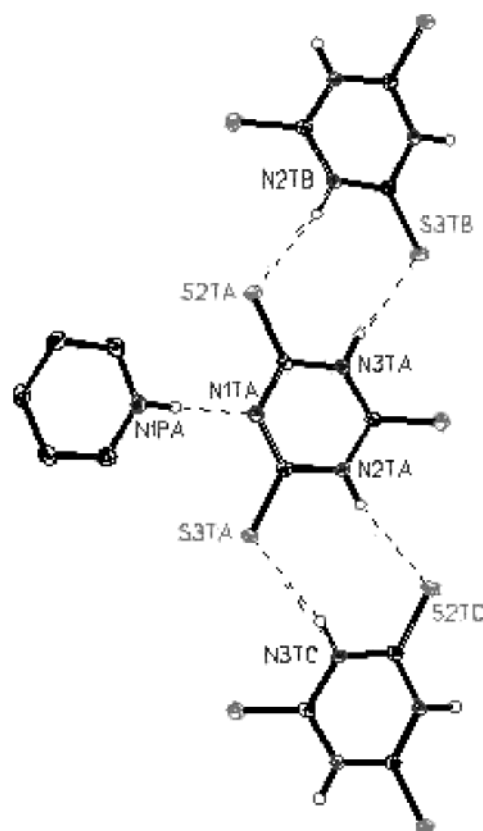


**Figure 10.** Structure of **5**. The relatively weak base, pyridine, in compound **5** deprotonates only a portion of the TMT. The remaining pyridine hydrogen-bonds to the N–H of the TMT ring. This is consistent with the base strength of the amine versus the base strength of the TMT.

the resulting crystals were removed for single-crystal analysis. Then, continued evaporation at an increased rate by loosely covering the beakers with aluminum foil produced precipitate for other analyses. The yields of the products were calculated on the basis of the specific reaction's limiting reagent, ratio of amine to H<sub>3</sub>TMT, and stoichiometry.

**[pyrrolidineH]<sup>+</sup><sub>2</sub>[HTMT]<sup>2-</sup>·THF (**1**).** To two beakers of stock solution were added 0.975 and 1.462 mL of the amine to H<sub>3</sub>TMT for 2:1 and 3:1 mixtures. Upon mixing, the 2:1 and 3:1 solutions turned a lemon yellow to a light yellow-brown with the formation of a precipitate and small crystals. After a portion of the solution evaporated, crystals formed that were large enough for single-crystal analysis. Both solutions resulted in the same product. Theoretical yield (actual yield):

1.85 g (1.34 g, 72% [2:1]; 1.44 g, 78% [3:1]). Mp (sealed capillary): 140–215 °C dec. Anal. (Calcd) found for [pyrrolidineH]<sup>+</sup><sub>2</sub>[HTMT]<sup>2-</sup>: C, (41.63) 40.32; H, (6.04) 6.56; N, (22.08) 21.61; S, (30.25) 30.01. IR (KBr, cm<sup>-1</sup>): 3442 mbr, 3095 s, 2959 s, 2914 s, 2750 m, 2629 w, 2570 w, 2447 w, 1546 s, 1490 s, 1457 s, 1399 s, 1336 m, 1223 m, 1135 s, 1025 w, 871m, 860 m, 772 w, 496 m, 459 m.

[(triethylamine)H]<sup>+</sup><sub>2</sub>[HTMT]<sup>2-</sup>·THF (2). To three beakers of stock solution were added 0.814, 1.628, and 2.44 mL of the amine to make 1:1, 2:1, and 3:1 mixtures. Upon mixing, all three solutions were very light yellow-brown and clear. After a portion of the solution evaporated, crystals formed that were large enough for single-crystal analysis. Identical products formed in all three solutions. Theoretical yield (actual yield): 1.62 g (1.06 g, 65% [1:1]; 1.21 g, 75% [2:1]; 1.05 g, 65% [3:1]). Mp (sealed capillary): 192–199 °C dec (into a liquid and a yellow solid). Anal. (Calcd) found for [(triethylamine)H]<sup>+</sup><sub>2</sub>[HTMT]<sup>2-</sup>: C, (38.84) 38.80; H, (6.52) 6.55; N, (20.14) 20.00; S, (34.49) 34.55. IR (KBr, cm<sup>-1</sup>): 3440 wbr, 3099 s, 2977 s, 2908 s, 2666 w, 2485 w, 2120 w, 2019 w, 1582 m, 1531 s, 1491 s, 1470 s, 1440 s, 1394 m, 1345w, 1325 s, 1256 m, 1233 s, 1136 s, 1031 w, 881m, 810 w, 716 w, 487 m, 468 m.

[(propylenediamine)H]<sub>2</sub><sup>2+</sup>[HTMT]<sup>2-</sup> (3). To a beaker of stock solution was added 0.489 mL of the amine. Upon mixing, the 1:1 solution was clear and very light yellow, with a fine white-yellow precipitate beginning to form. After a portion of the solution evaporated, crystals formed that were large enough for single-crystal analysis. Theoretical yield (actual yield): 1.47 g (0.66 g, 45%). Mp (sealed capillary): melted and then sublimed at 190 °C. Anal. (Calcd) found for [(propylenediamine)H]<sub>2</sub><sup>2+</sup>[HTMT]<sup>2-</sup>: C, (28.68) 28.95; H, (5.22) 5.40; N, (27.89) 27.89; S, (38.21) 39.34. IR (KBr, cm<sup>-1</sup>): 3437 mbr, 3099 s, 2920 sbr, 2644 w, 2049 w, 1592 w, 1507 s, 1437 s, 1340 w, 1319 m, 1255 m, 1205 s, 1132 s, 1078 w, 1011 w, 956 w, 895 w, 861 m, 817 w, 752 w, 493 w, 483 w.

[(ethylenediamine)H]<sub>2</sub><sup>2+</sup>[HTMT]<sup>2-</sup> (4). To a beaker of stock solution was added 0.390 mL of the amine. After mixing, the 1:1 solution was white and slightly opaque with a fine precipitate forming. After a portion of the solution evaporated, crystals formed that were large enough for single-crystal analysis. Theoretical yield (actual yield): 0.867 g (0.615 g, 71%). Mp (sealed capillary): went from a light yellow to orange by 140 °C and red-black at 300–330 °C and melted into a black tar at 343 °C. Anal. (Calcd) found for [ethylenediamineH]<sub>2</sub><sup>2+</sup>[HTMT]<sup>2-</sup>: C, (28.27) 28.06; H, (6.45) 6.00; N, (32.99) 31.02; S, (32.29) 32.36. IR (KBr, cm<sup>-1</sup>): 3406 wbr, 3117 s, 2949 s, 2054 w, 1559 m, 1499 s, 1433 s, 1326 m, 1266 w, 1202 s, 1132 m, 1056 w, 987 w, 870 m, 746 w, 664 w, 486 w.

[(pyridine)H]<sup>+</sup><sub>2</sub>[HTMT]<sup>2-</sup>·(H<sub>3</sub>TMT·2(pyridine)) (5). To three beakers of stock solution were added 0.472, 0.945, and 1.417 mL of the amine to make 1:1, 2:1, and 3:1 mixtures. After mixing, all three solutions were clear, light pale yellow, growing slightly darker yellow from 1:1 to 3:1. After a portion of the solution evaporated, crystals formed that were large enough for single-crystal analysis. Identical products formed in all three solutions. Theoretical yield (actual yield): 0.8446 g for [1:1] and 1.267 g for [2:1 and 3:1] (0.82 g, 97% [1:1]; 0.82 g, 65% [2:1]; 0.96 g, 76% [3:1]). Mp (sealed capillary): crystals turned opaque at 130 °C and slowly decomposed to a rich brown color from 290 to 330 °C. Anal. (Calcd) found for [(pyridine)H]<sup>+</sup><sub>2</sub>[HTMT]<sup>2-</sup>·(H<sub>3</sub>TMT): C, (30.42) 31.62, H, (2.79) 2.61, N, (22.59) 22.54, S, (44.21) 44.25. IR (KBr, cm<sup>-1</sup>): 3452 wbr, 3122 m, 3037 m, 2877 m, 2679 w, 2563 w, 2019 w, 1583 m, 1554 s, 1483 m, 1379 s, 1246 m, 1143 s, 1034 w, 889 w, 753 m, 695 w, 676 m, 490 w, 459 m.

**Acknowledgment.** This work was supported by the National Science Foundation NSF-CAREER award

(Grant No. CHE 9625376). NMR instruments used in this research were obtained with funds from the CRIF program of the National Science Foundation (Grant No. CHE 997841) and from the Research Challenge Trust Fund of the University of Kentucky.

**Supporting Information Available:** Crystallographic data for compounds 1–5, which includes full tables of bond lengths and angles, fully labeled ORTEP drawings, unit cell views, and observed and calculated structure factor tables. This material is available free of charge via the Internet at <http://pubs.acs.org>. These data may also be obtained from the Cambridge Crystallographic Database (CCDC).

## References

- Lehn, J.-M. *Supramolecular Chemistry*; VCH: Weinheim, Germany, 1995.
- Steed, J. W.; Atwood, J. L. *Supramolecular Chemistry*; Wiley: New York, 2000.
- Mattes, R.; Weber, H. *J. Chem. Soc., Dalton Trans.* **1980**, 423.
- Belaj, F.; Tripolt, R.; Nachbaur, E. *Monatsh. Chemie* **1990**, 121, 99.
- Cea-Olivares, R.; Jimenez-Sandoval, O.; Hernandez-Ortega, S.; Sanchez, M.; Toscano, R. A.; Haiduc, I. *Heterocycl. Chem.* **1995**, 6, 89.
- Allen, F. H.; Bird, C. M.; Rowland, R. C.; Raithby, P. R. *Acta Crystallogr.* **1997**, B53, 680–695, 696–701.
- Ueyama, N.; Yamada, Y.; Okamura, T.; Kimura, S.; Nakamura, A. *Inorg. Chem.* **1996**, 35, 6473.
- Simanek, E. E.; Isaacs, L.; Li, X. H.; Wang, C. C. C.; Whitesides, G. M. *J. Org. Chem.* **1997**, 62, 8994.
- Henke, K. R.; Hutchison, A.; Krepps, M. K.; Atwood, D. A. *Inorg. Chem.*, in press.
- Loughran, G. A.; Ehlers, G. F. L.; Crawford, W. J.; Burkett, J. L.; Ray, J. D. *Appl. Spectrosc.* **1964**, 18, 129.
- Chudy, J. C.; Dalziel, A. W. *J. Inorg. Nucl. Chem.* **1975**, 37, 2459.
- Bailey, J. R.; Hatfield, M. J.; Henke, K. R.; Krepps, M. K.; Morris, J. L.; Otieno, T.; Simonetti, K. D.; Walls, E.; Atwood, D. A. *J. Organomet. Chem.* **2001**, 623, 185.
- Kopel, P.; Travnicek, Z.; Kvittek, L.; Panchartkova, R.; Biler, M.; Marek, J.; Nadvornik, M. *Polyhedron* **1999**, 18, 1779.
- Tiainen, H.; Krepps, M. K.; Henke, K. R.; Hutchison, A.; Laitinen, R. S.; Matlock, M. M.; Atwood, D. A. To be submitted for publication.
- Francois, S.; Rohmer, M.-M.; Benard, M.; Moreland, A. C.; Rauchfuss, T. B. *J. Am. Chem. Soc.* **2000**, 122, 12743.
- Jeyagowry, K. S.; Sampanthar, T.; Vittal, J. J. *Inorg. Chim. Acta* **1999**, 295, 7.
- Henke, K.; Atwood, D. A. *Inorg. Chem.* **1998**, 37, 224.
- Hunter, C. A.; Sanders, J. K. M. *J. Am. Chem. Soc.* **1990**, 112, 5525.
- Harris, K. D. M.; Stainton, N. M.; Callan, A. M.; Howie, R. A. *J. Mater. Chem.* **1993**, 3, 947.
- Adman, E.; Watenpugh, K. D.; Jensen, L. H. *Proc. Natl. Acad. Sci. U.S.A.* **1975**, 72, 4854.
- Sheldrick, G. M. SHELX97: Programs for Crystal Structure Solution and Refinement; University of Gottingen, Gottingen, Germany, 1997.
- International Tables for Crystallography*, Hahn, T., Ed.; Kluwer Academic: Dordrecht, The Netherlands; Vol A (Space Group Symmetry).
- Parkin, S. *Acta Crystallogr.* **2000**, A56, 157.